INTERNATIONAL TRANSACTIONS ON ELECTRICAL ENERGY SYSTEMS
Int. Trans. Electr. Energ. Syst. 2015; **25**:933–947
Published online 7 February 2014 in Wiley Online Library (wileyonlinelibrary.com). DOI: 10.1002/etep.1869

Computing sensitivities from synchrophasor data for voltage stability monitoring and visualization

Rujiroj Leelaruji[1]*,†, Luigi Vanfretti[1,3], Kjetil Uhlen[2] and Jan Ove Gjerde[3]

[1]*Royal Institute of Technology, KTH, Electric Power Systems, Sweden,*
[2]*Norwegian University of Science and Technology (NTNU), Electrical Power Engineering, Norway,*
[3]*Statnett SF, Research and Development, Norway*

SUMMARY

Wide-area early warning systems are dependent on synchrophasor data-based applications for providing timely information to operators so that preventive actions can be taken. This article proposes the use of voltage sensitivities computed from synchrophasor data for voltage stability monitoring, and a visualization approach that can be implemented in wide-area early warning systems. In order to provide reliable information, this article addresses the issue of data filtering and correction and proposes a filtering methodology for robust voltage sensitivity computation. The methodology is developed considering both positive-sequence simulations for methodology development purposes, and *real* phasor measurement data from a real-time (RT) hardware-in-the-loop (HIL) laboratory for testing the robustness of the developed approach under more realistic conditions. The limitations of the positive-sequence simulation approach for developing phasor measurement unit (PMU)-data applications are highlighted, and the challenges of working with the RT-HIL lab are recognized. The proposed sensitivity computation approach has also been applied to a real PMU-data obtained from the Nordic transmission system where results are sustained. Copyright © 2014 John Wiley & Sons, Ltd.

KEY WORDS: wide-area voltage instability detection; wide-area monitoring systems; wide-area early warning systems; visualization; PMU-based applications; filtering

1. INTRODUCTION

Phasor measurement units (PMUs) have been adopted to provide a high-sampling rate positive-sequence voltage and current phasors for wide-area monitoring, protection and control (WAMPAC) systems [1]. The successful deployment of PMUs [2] and applications that harvest their data in WAMPAC systems have the potential of gradually transforming today's power transmission networks into smart transmission grids [3]. Within WAMPAC systems, wide-area early warning systems are dependent on synchrophasor data-based applications for providing timely information to operators so that preventive actions can be taken.

As recognized in [3], the development and deployment of PMU-data-based applications have been slow, limiting the potential of WAMPAC systems. Nevertheless, to date, a number of applications have been implemented in industrial wide-area monitoring systems (WAMS), mainly to provide awareness to disruptive events. The use of these applications is catered, for example, to provide the wide-area visibility [4,5], the detection of critical oscillatory mode properties [6,7] and the voltage instability detection [8]. Note that the design of WAMS and WAMPAC systems in general also includes the possibility for implementing other applications [9].

Most of the voltage instability detection methods that have been proposed, with two notable exceptions [10,11], rely upon the construction of Thévenin equivalent models with synthesized parameters. Although useful and reliable, these methods have limitations which have been recognized in [11,12].

*Correspondence to: Rujiroj Leelaruji, Electric Power Systems, Royal Institute of Technology, KTH, Sweden.
†E-mail: rujiroj@kth.se

With "wide-area methods" [10,11], the use of sensitivities may have great potential for detecting the inception of voltage instabilities in wide areas without depending on circuit synthesis. However, the computation of sensitivities from synchronized phasor-measurement data has several challenges.

First, the development of most voltage stability (VS) monitoring methods has been traditionally carried out through positive-sequence-based (PSB) models and simulations. This is reasonable in principle as the time scale of this type of instability is, in most cases, larger in comparison to other types of instabilities [13]. However, it has the disadvantage that the synthetic data generated by the simulation of these models does not contain the actual features that one expects from actual PMU-data, nor does it deal with the possible data errors and inconsistencies embedded in synchrophasor streams. A lack of and/or incorrect data processing can yield incorrect information, which can mislead operators to take non-optimal preventive actions, or even an improper action that could lead to a collapse.

This article proposes the use of voltage sensitivities computed from synchrophasor data for VS monitoring, and a visualization approach that can be implemented in wide-area early warning systems. A filtering methodology for robust voltage sensitivity computation is proposed. The methodology is developed considering both positive-sequence simulations, and *real* phasor measurement data from a real-time (RT) hardware-in-the-loop (HIL) laboratory for testing the robustness of the developed approach in control room applications. The limitations of the positive-sequence simulation approach for developing PMU-data applications are highlighted, and the challenges of working with the RT-HIL lab are recognized. The proposed sensitivities have also been applied to a real PMU-data obtained from the Nordic transmission system where results are sustained.

2. WIDE-AREA VS MONITORING CONCEPTS

Voltage instability detection methods can be categorized in to the following branches: local [14,15] versus wide-area measurement [16] or synchronized [17] versus non-synchronized [18] approaches. The idea behind these categories is on how the accumulated measurement information is used. To have an complete system awareness, it appears that the entire power system state needs to be reconstructed from synchrophasor measurements and other data [19], or that different indices for different system components need to be computed to determine instabilities [17]. It can be argued that wide-area early warning systems could contain monitoring tools that display VS indicators; however, it is not clear how to present this information to operators so that it is easy to understand. Therefore, the ultimate goal of this article is to create the VS indicators by computing sensitivities that are simple to comprehend.

PMU-data must be first pre-processed in order to compute accurate and robust sensitivities if they are to be used for control room applications. This issue is avoided in [10] by extracting the slope of the sensitivities instead of sensitivities themselves. To achieve this, a parcel of data is needed, delaying the delivery of information to a wide-area early warning system. The pre-processing issue is partly addressed in [12] by using filtering to separate the quasi-steady state components of simulated data; however, the approach is limited because the simulated data does not contain the correct features observed from PMU-data and it is not capable to cater for inconsistencies and errors embedded in them. Hence, a filtering methodology for robust voltage sensitivity computation is proposed in Section 4.

3. PV AND QV SENSITIVITIES AS VS INDICATORS

The use of voltage sensitivities for voltage instability detection has been proposed in [11,20,21,10]. In this study, a similar approach is adopted; however, a different Jacobian matrix from that of the standard power flow problem is utilized. First, individual components of sensitivities are constructed from the power flow in each transmission line (one direction) instead of injected power flow of the bus (summation of power flow). Second, the lines' power flow is calculated solely based on measured voltage and current phasors. This means that the effects of shunt capacitances of the transmission line (in the case of medium and long lines) of the nominal π-model are also included.

DOI: 10.1002/etep

The transmitted power on the line can be expressed as follows:

$$\begin{aligned} \overline{S}_{ik} &= V_i e^{j\delta_i}\left\{I_{ik}e^{j\delta_{ik}}\right\}^* \\ P_{ik} = Re\left(\overline{S}_{ik}\right), &\qquad Q_{ik} = Im\left(\overline{S}_{ik}\right) \end{aligned} \tag{1}$$

where

V_i = voltage magnitude at Bus i.

I_{ik} = current magnitude from from Bus i to Bus k.

δ_i = voltage angle at Bus i where $\delta_{ik} = \delta_i - \delta_k$

$\overline{S}_{ik}$ = complex power transmitted from Bus i to Bus k.

P_{ik} = transmitted real power from Bus i to Bus k.

Q_{ik} = *transmitted reactive power from* Bus i to Bus k.

From Equation 1, it follows that the real and reactive power flows through the transmission lines can be calculated directly regardless the system's parameters (different from [11,12]). Normally, sensitivities in Jacobian matrix are constructed as a production of partial derivatives; however, these proposed sensitivities are computed discretely as the ratio of differences in two consecutive computation points from measured voltages and powers which are constructed as follows:

$$\text{Sensitivities} \Rightarrow \begin{bmatrix} \delta_{P_{ik}}(t) & V_{P_{ik}}(t)(2) \\ \delta_{Q_{ik}}(t) & V_{Q_{ik}}(t) \end{bmatrix} \tag{2}$$

where

$$\begin{aligned} \delta_{P_{ik}}(t) &= \delta_i(t) - \delta_i(t-1)/P_{ik}(t) - P_{ik}(t-1) = \Delta\delta_i/\Delta P_{ik} \\ V_{P_{ik}}(t) &= V_i(t) - V_i(t-1)/P_{ik}(t) - P_{ik}(t-1) = \Delta V_i/\Delta P_{ik} \end{aligned}$$

Similar expressions can also be derived for $\delta_{Q_{ik}}$ and $V_{Q_{ik}}$.

In this paper, only $\Delta V_i/\Delta P_{ik}$, and $\Delta V_i/\Delta Q_{ik}$ are studied and used as voltage instability indicators. Each individual component of sensitivities is obtained from the PMU-data. The values of these sensitivities can aid in assessing voltage instability with the considerations below.

(1) The sensitivities are consistently at a low-positive value (or negative depending the current measurement direction) with the assumption of steady-state operation. This indicates that a system operates far away from a voltage instability condition.
(2) The value of the sensitivities will increase positively (or negatively) when a system is stressed. This denotes a system is moving towards a "weak" operating condition; thus, this is a trend in the development of the voltage instability.
(3) The value increases abruptly to very high positive (or negative) and switches sign in the case of a lack of reactive power support for $\Delta V_i/\Delta Q_{ik}$ or when the maximum power transfer is reached for $\Delta V_i/\Delta P_{ik}$. This depicts an unstable condition which consequently leads to voltage collapse.

A graphical example and the methodology to use these sensitivities to detect voltage instability and generate either an early warning alarm or a final alarm are illustrated in Sections 4 and 6, respectively.

4. FILTERING METHODOLOGY

The proposed filtering method used in this study is similar to the low pass-part of the complementary filter in [22]. There are two restrictions that differentiate this filter from an ordinary low pass filter[1] which is affected by discrete events occur in power systems. Therefore, this filter screens out only a

[1] 1) the high pass filter must have left-right symmetry (i.e. a zero or linear phase), and 2) the impulse must be added at the center of symmetry [23].

DOI: 10.1002/etep

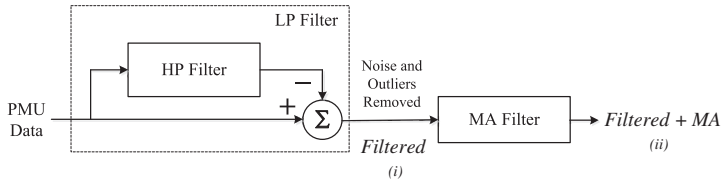

Figure 1. Proposed filtering approach for pre-processing data to compute voltage stability indicators.

high frequency noise. Its aim is to smooth all signals before computing voltage sensitivities. Figure 1 shows a block diagram of the processing method. It starts by taking raw data and applying a first-order high pass filter with cutoff frequency of 1.37 Hz. This cutoff frequency corresponds to the dominant oscillatory component in the system. Then, the original data is subtracted by the filtered data. By applying this subtraction, electromechanical oscillations and large outliers are removed from the original signal; this is shown in Figure 1 with a (*i*); signals from this step are termed "*Filtered*" signals.

There are two ways to filter the signal which are "*post-event*" and "*near real-time*" approaches. In the *post-event* approach, the time-synchronized data is gathered from different locations for a particular time range, and the entire set of data is filtered. Here, the start-up and ending transients of the filters are minimized by matching the initial and final conditions. This is accomplished by reversing the filtered data sequence and processing the input data in both the forward and reverse directions. On the other hand, the "*near real-time*" approach processes the input data only in the forward direction. The start-up and ending transients for this approach can be eliminated by buffering data into a predefined finite-size window. The data buffer for eliminating the start-up transient can be constructed by creating parcels[2] which contains the steady-state values of each variable.[3] Then, the data in the buffer is replaced with measurements, one sample at a time, always maintaining the finite-size window full. The filtering process is applied to each window data, which is updated with each new sample. Finally, the ending transient of the filter is eliminated by using the last measured samples in a data buffer to maintain the size of window data (in a similar fashion as described for the other parcels used).

An additional step is to apply a moving average (MA) window by computing the mean and standard deviation of the filtered signal. The size of the MA window is designed to cover the data which deviates from the mean value by three standard deviations of the filtered signal, which originally has the same size as the predefined finite-size window mentioned earlier. Then, this predefined finite size of the MA window is decreased when MA algorithm detects the data exceeds the threshold standard deviation. This process is repeated over the entire data set. As denoted in Figure 1 (*ii*), these signals are termed "*Filtered + MA*". The MA aids to increase the robustness of the computed sensitivities. This filtering method is applied to both the DIgSILENT PowerFactory simulation (of 0.001 s step-size) and the PMU measurement data (50 samples per second).

5. EXPERIMENTAL AND SIMULATION SETUPS

5.1. Test system

A one-line diagram of the test system is shown in Figure 2. The system consists of a local area connected to a strong grid (Thevenin Equivalent) by two 380 kV transmission lines. A motor load (rated 750 MVA, 15 kV) is connected at Bus 4 and supplied via a 380/15 ratio transformer. A load with constant power characteristics and on-load tap changer (OLTC) dynamics at the distribution side are explicitly modelled at Bus 5. A local generator (rated 450 MVA, 20 kV) equipped with a simplified IEEE ST1A excitation system, a standard speed-governing model and a simplified linear model of steam turbine is connected at Bus 2 to supply the loads through a 20/380 ratio transformer. The load at Bus 5 is equipped with an automatic discrete OLTC. This system is capable of reproducing different instability scenarios. However,

[2]This parcel is a vector of data which contain in each entry the steady-state values of its corresponding variable.
[3]When using models, this steady-state value can be obtained from the power flow solution.

DOI: 10.1002/etep

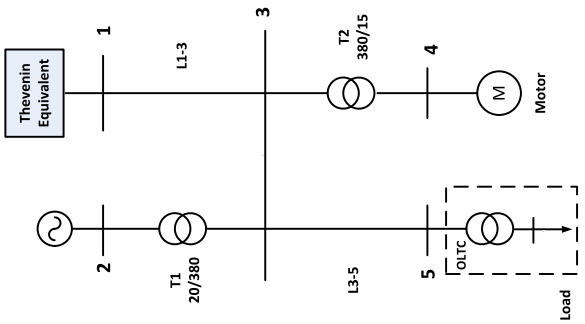

Figure 2. Test system used for generating voltage instability scenarios.

only voltage instabilities are the focus of this paper. More details regarding components' modeling and other instabilities that can be reproduced by this system can be found in [24].

5.2. PSB simulations versus "real" PMU-data

The reason of having the test system in two test platforms (PSB simulations and RT-HIL) is to guarantee that the proposed sensitivities are robust enough to us as a monitoring tool when the "real" PMU-data is involved. This is because PSB simulations may exclude the effect of switching devices and events on measurements, ambient behavior, noise and outliers in actual PMU-data.

Since it is costly to adopt a real power system for experimental purposes, an experimental testing platform that performs as close as possible to real existing networks is adopted for the experiments involving *real* PMU-data. In this paper, we consider only one aspect of the problem by having PMUs in the loop. Several practical aspects such as problems in communications (e.g. package delay) or impact of measurement channels (e.g. PTs, CTs, measurement cables) are not considered but will be described in future publication. A brief summary on how PMU RT-HIL data is generated can be found in [25].

5.3. Study cases

The voltage instability scenario used for demonstration is implemented by increasing the load at Bus 5 of the test system shown in Figure 2. Typical constant active and reactive power models are used. The load is assumed to change as follows:

$$P_L = P_{Lo}(1 + \lambda) \tag{3}$$

$$Q_L = Q_{Lo}(1 + \beta) \tag{4}$$

where P_{Lo} and Q_{Lo} are the initial base active and reactive powers, respectively, and λ and β are varying parameters representing the active and reactive loading factors, respectively.

Case 1 **Load increase without OEL**

Case 1.1 **PSB simulation**As mentioned earlier, the load at Bus 5 is increased at $t = 70$ s. The OLTC tries to restore the voltage at the load bus within its deadband [26]. Since the load increases monotonically, the OLTC unsuccessfully attempts to restore the load bus voltage, until it reaches its lower limit. The load bus voltage then decreases stepwise accordingly and the system collapses at $t = 440$ s (see Figure 3).

The filtering approach and sensitivities computation (as described in Sections 4 and 3, respectively) are applied in order to demonstrate advantages of the proposed method. Figures 3 and 4 show the difference between filtering and not filtering a voltage and the corresponding PV-curve at Bus 5, respectively. Figure 5 depicts the plot of a sensitivity ($\Delta V_5/\Delta P_{53}$) at Bus 5 that was obtained by using data from a DIgSILENT PowerFactory PSB simulation.

DOI: 10.1002/etep

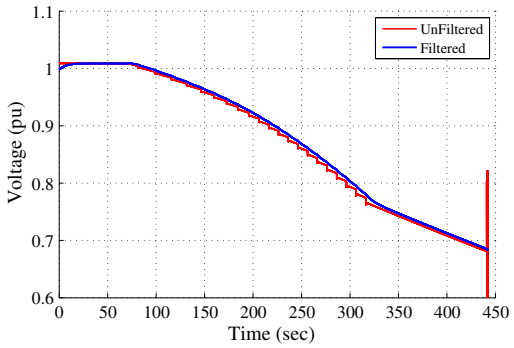

Figure 3. Filtered and unfiltered voltage at Bus 5 (PSB simulation).

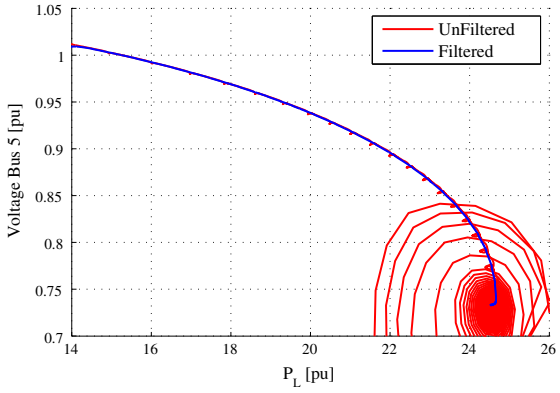

(a) PV-curve (Load Power vs Voltage Bus 5)

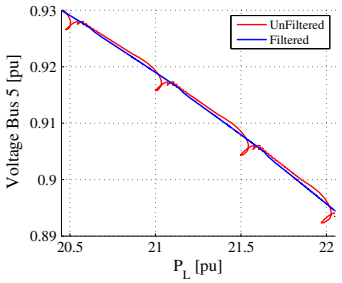

(b) Zoom of Fig. 4a

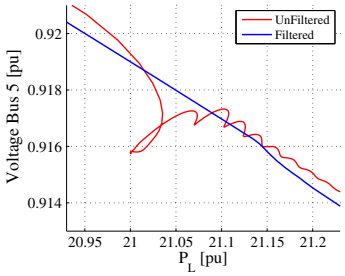

(c) Zoom of Fig. 4b

Figure 4. Filtered and unfiltered PV-curve (PSB simulation).

As mentioned in Section 3, the sensitivity ($\Delta V_i/\Delta P_{ik}$ in this case) can be used to generate an early warning alarm when its value changes from positive to negative; this occurs at $t = 400$ s (while the system collapses at $t = 440$ s). This early warning alarm can be generated by setting a threshold value (e.g. $\Delta V_5/\Delta P_{53} = 0.08$); this allows detection before the sensitivity changes abruptly to a large positive value. This can be verified from Figure 3. The spikes shown in the green in Figure 5 correspond to OLTC tap position changes. It can also be noted that the sensitivity calculated from the unfiltered data (green dashed line) are vulnerable to OLTC tap switching and vary abruptly compared with those computed using data which has been filtered, or filtered with MA. Figure 6 shows that the "filtered + MA" approach provides a more robust result compared to the one without MA. However, these filtering methods

DOI: 10.1002/etep

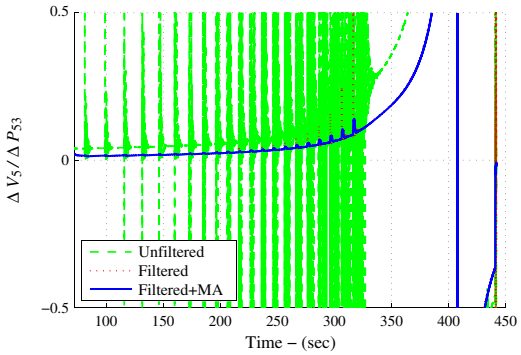

Figure 5. Plot of calculated $\Delta V_5/\Delta P_{53}$ sensitivity at Bus 5 from filtered PSB simulation data.

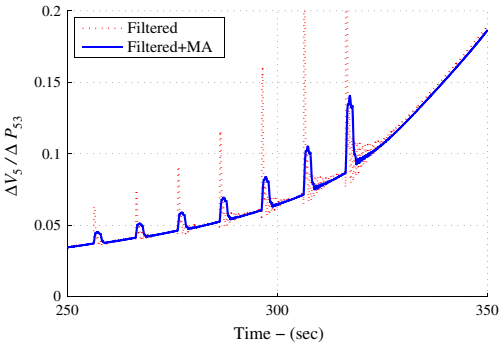

Figure 6. Zoom of Figure 5 (without unfiltered data plot.

(either with or without MA window) introduce a small delay to the calculation (≈5 s for this experiment).

Case 1.2 **RT-HIL simulation**The same experiment is conducted in the laboratory using the RT-HIL approach, and the synchrophasors for Bus 5 are acquired. Figure 7 shows the voltage magnitude from the phasor streamed out from a SEL PMU. Note that the traces obtained from the PMU have a higher resolution than those from the PSB simulation (Figure 3). Notice that Figure 7 clearly contains not only electromechanical oscillations, but also noise, and outliers due to the switching of discrete devices whereas Figure 3 does not contain most of these characteristics. To develop a robustwide-area monitoring application, these data features need to be considered.

Similar results were obtained using PMU-data, which are shown in Figure 8. Here, the spikes due to OLTC switching that appear in the computed sensitivities are much higher than those obtained using PSB simulation results. This is of natural occurrence with measurement devices when sampling a signal that has been subject to discrete switching. Moreover, there are other nuisances in the PMU-data generated from the RT-HIL simulator such as outliers and noise. The "filtering + MA" approach helps in dealing with these natural characteristics of measurement data.

In addition, the voltage when the system becomes unstable for Case **1.1** is lower compared with of Case **1.2**. This is because the load in Case **1.1** is modeled as constant impedance characteristic which leads to the collapsing point not necessary to be at the tip of the PV-curve but it can be at very low voltage value [27] (see Figure 4). This means that the lower part of the PV-curve, which indicates an unstable region, can be drawn before

DOI: 10.1002/etep

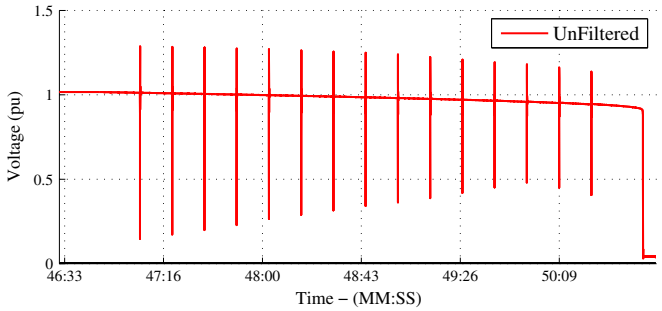

(a) Voltage Magnitude at Bus 5 - complete time span until collapse.

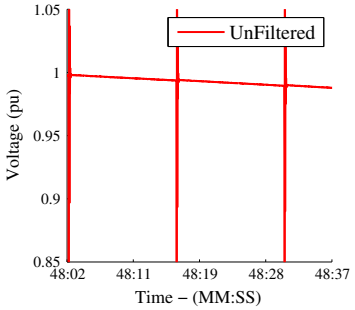

(b) Zoom of Fig. 7a

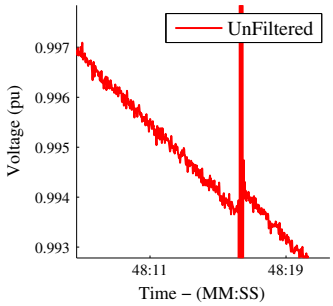

(c) Zoom of Fig. 7b

Figure 7. Voltage magnitude at Bus 5 from PMU measurements.

reaching instability limit. Meanwhile, the load in Case **1.2** is modeled as constant power characteristic where the tip of the PV-curve represents both the maximum loadability and voltage instability limit [27]. The intention of having constant power load is to verify that the proposed sensitivities can detect a voltage collapse whether the voltage level is not at low values or if the lower part of the PV-curve does exist as with constant impedance loads. Therefore, sensitivities only increase abruptly to very high positive but do not switch sign as in Case **1.1**.

Case 2 **Load tripping with OEL limit**In this test scenario, an over excitation limiter (OEL) is added to allow a generator to operate at high excitation levels for a sustained duration. An OEL is adopted to suppress the field current for cases when the temperature of the field winding exceeds the allowed level. The test system (shown in Figure 2) is modified by adding a transmission line parallel to L1-3. A modification is done so that the total impedance of these lines equals to the same as in the original system.

A voltage instability is created by tripping one of the parallel lines between Bus 1 and Bus 3. The generator at Bus 2 produces more power to compensate the power flow from the Thevenin equivalent due to disconnected line. As seen in Figure 9, the OLTC also attempts to restore the load bus voltage; however, an OEL at the generator is activated (at "●"). Consequently, the generator voltage is no longer controlled and the voltage at Bus 5 drops steeply as shown in Figure 9. Figure 10 also shows that the OLTC attempts to restore the load bus voltage to the initial load condition (represented by the vertical dash-dot line). However, when OEL's limit is reached, the system's operating point jumps from one PV-curve (at "●") to another PV-curve ("♦") where there is no intersection between the PV-curve and the load, thus the system is unstable.

The $\Delta V_i/\Delta Q_{ik}$ (see Figure 11) is of interest due to coupling between voltage and reactive power. After the OEL's limit is reached, it can be seen that the $\Delta V_5/\Delta Q_{53}$ increases sharply and switches from positive values to negative ones.

DOI: 10.1002/etep

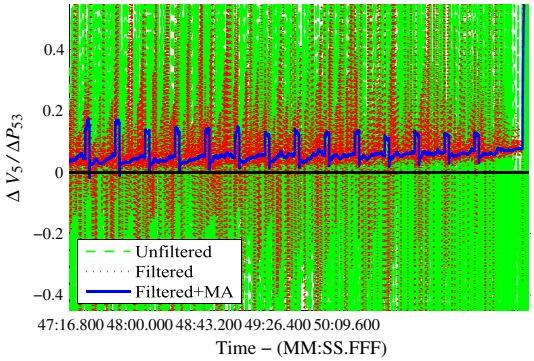

(a) Plot of calculated $\Delta V_5/\Delta P_{53}$ sensitivity using PMU-data.

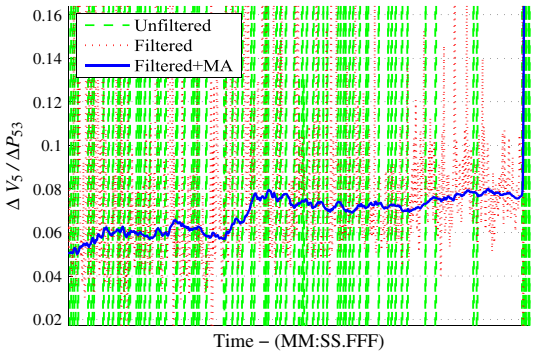

(b) Zoom of Fig. 8a when $\Delta V_5/\Delta P_{53}$ changes abruptly

Figure 8. $\Delta V_5/\Delta P_{53}$ sensitivity using PMU-data generated from the RT-HIL experiment.

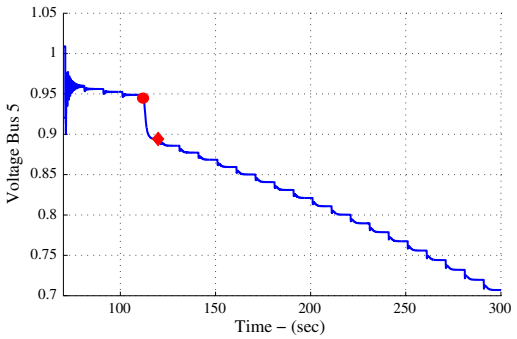

Figure 9. Voltage at Bus 5: OEL limit case.

Case 3 **Real PMU-data from the Nordic grid**In this case, the PMU-data from 29 January 2010 was gathered from three PMUs installed in the Nordic grid. Figure 12 shows PMUs located at high voltage substations.

Figure 13 shows measured voltage from three substations, and Figure 14 depicts only the filtered voltage of the "North" substation obtained by applying the filtering method described in Section 4.

As seen in Figure 14, the voltage at "North" substation started to drop at 16:07 h and one of the transmission lines near the substation was disconnected at 16:10 h. The OLTC was activated to step up the voltage level at 16:12 h and 16:15 h, respectively. However, since the voltage was very low

DOI: 10.1002/etep

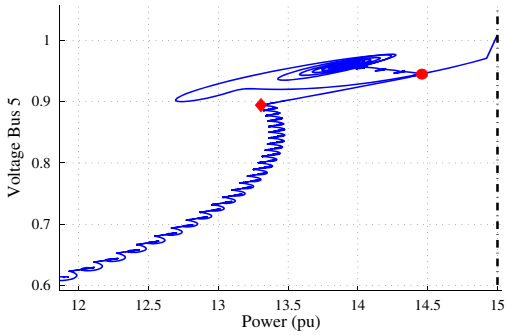

Figure 10. PV-curve: OEL limit case.

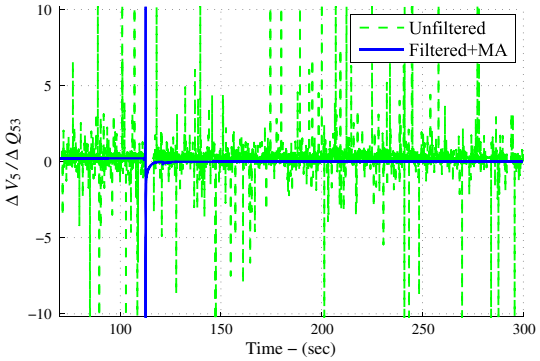

(a) Plot of calculated $\Delta V_5 / \Delta Q_{53}$ sensitivity

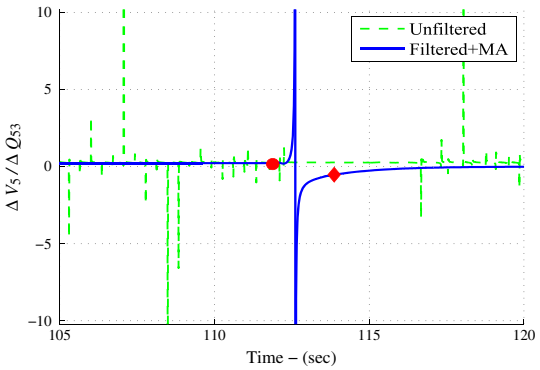

(b) Zoom of Fig. 11a

Figure 11. $\Delta V_5/\Delta Q_{53}$ sensitivity: OEL limit case.

(0.93 pu approximately), a large industrial load, which is located 160 km away from the mainland, was manually disconnected to prevent a voltage collapse. Figure 15 shows the $\Delta V_i/\Delta Q_{ik}$[4] sensitivity calculated from PMU-data of the "North" substation can detect the line tripping (indicated by "**1**"), the two steps of OLTC's activation ("**2**" and "**3**") and the load disconnection ("**4**"). The authors suspect that the $\Delta V_i/\Delta Q_{ik}$ sensitivity would increase steeply if the load was not shedded. In addition, it is worth

[4] ΔQ_{ik} is calculated from the measured reactive power flows in the line towards the large industrial load

DOI: 10.1002/etep

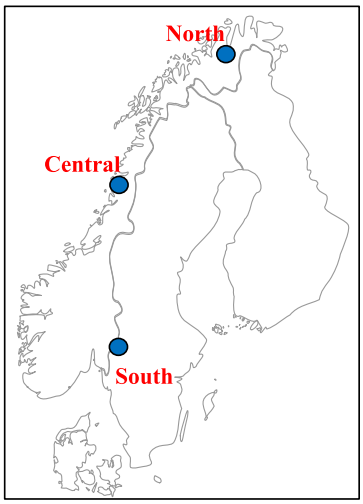

Figure 12. Nordic transmission system and approximate PMU locations.

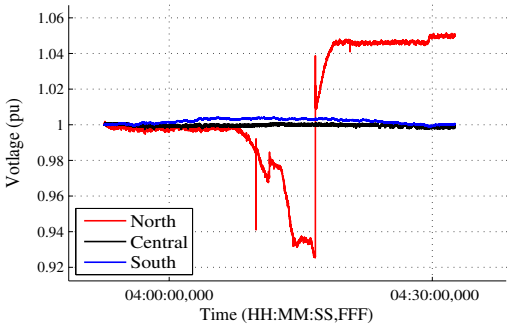

Figure 13. Measured voltage from three high voltage substations.

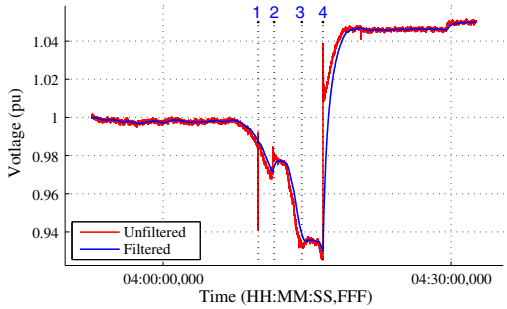

Figure 14. Unfiltered and filtered voltage of the "North" substation.

noting that the sensitivity decreases after the load disconnection and it remains at a positive value which means that the system is stable.

It has been proved that the proposed sensitivities are feasible for PSB simulation, RT-HIL and real PMU-data cases. Since individual sensitivities are reconstructed from measurements, there are many advantages obtained from this proposed method. First, power system or its topology changes are not required. Second, for short-term dynamics such as generator control and limits, e.g. OEL, although

DOI: 10.1002/etep

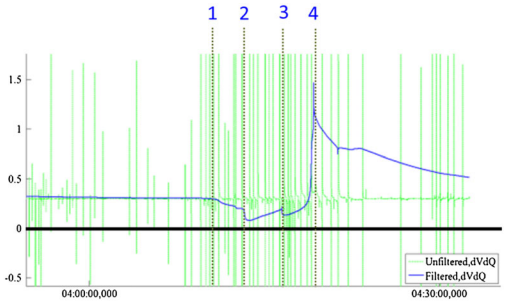

Figure 15. $\Delta V_i/\Delta Q_{ik}$ sensitivity calculated from PMU-data of the "North" substation.

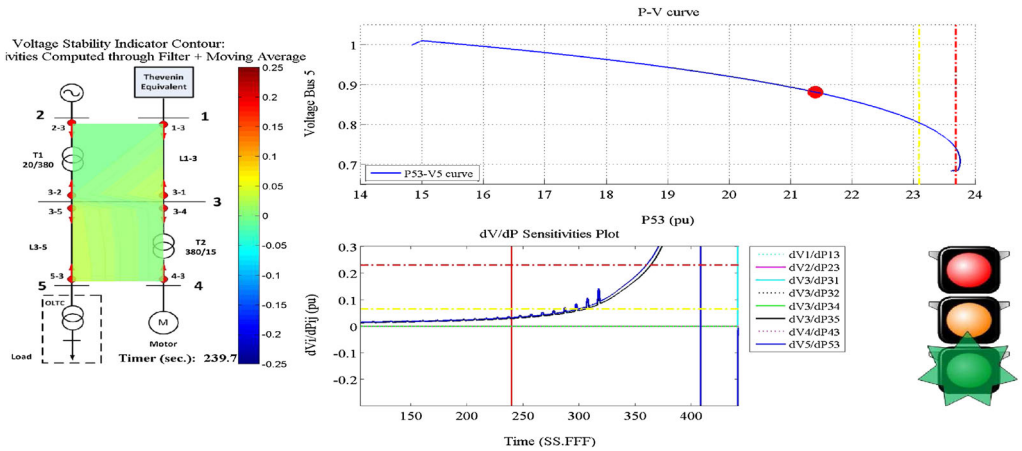

Figure 16. Screenshot of voltage stability monitor: $\Delta V_5/\Delta P_{53}$ sensitivities.

their actual control modes are not known by the methodology, it is possible to detect their change from the computed sensitivities. Also, the methodology is feasible for systems that consist of discrete switching components, e.g. OLTC, where unwanted noise and especially outliers exist.

6. VISUALIZATION APPROACH

For visualization purposes, the voltage phasors are gathered from different locations of the system shown in Figure 2. Each incoming voltage and current phasors from different locations is filtered as described in Section 4. Then, the active and reactive power flow of each line is calculated from 1. Consequently, sensitivities are computed as described in Section 3. The computed sensitivities for each location are assembled in one display which maps their values to a contour overlaying the power system one-line diagram.[5] Figure 16 shows a screenshot of the VS monitor tracking $\Delta V_5/\Delta P_{53}$ (Case **1.1** in Section 5.3). As shown in Figure 16, the contour is on the left-hand side while the sensitivities are displayed in the middle; a vertical red line indicates the time instant for which the contour is being computed. The top-right-hand side is the PV-curve of a particular bus chosen by the user. A red circle indicates the current operating condition, which has been computed from the PMU-data. Vertical and horizontal yellow and red dash–dot lines indicate the distance to the maximum power transfer (active power margin) for the $\Delta V_i/\Delta P_{ik}$ thresholds that have been set by user. These correspond to the "traffic signal" that is displayed on the bottom-right-hand side. The green light of this traffic signal

[5]Observe that this could also be done using a Geographical Information System (GIS).

DOI: 10.1002/etep

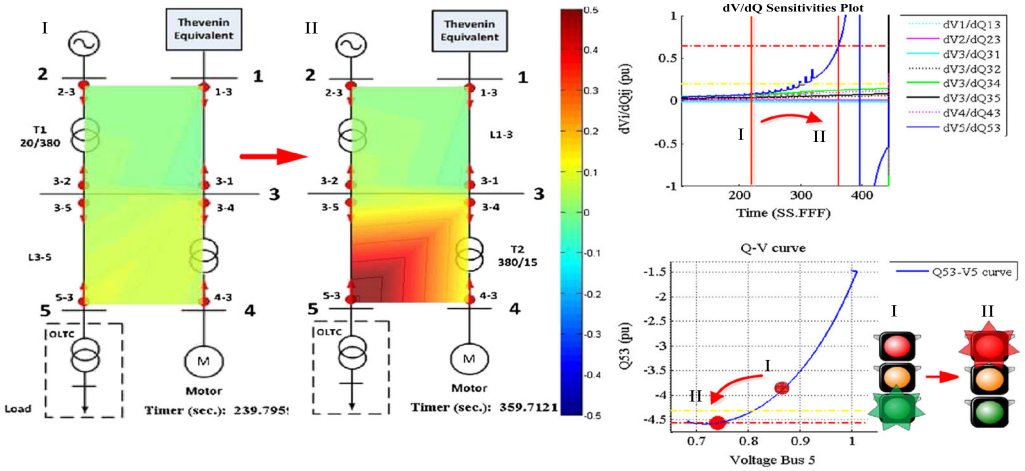

Figure 17. Transition of $\Delta V_5/\Delta Q_{53}$ sensitivities from $t = 240$ s to $t = 360$ s.

indicates the fact that the system is in a secure operating state while yellow and red refer to an insecure and an emergency state, respectively. Determination of the PV and QV curves and P & Q margins for each bus can be carried out off-line through continuation studies, or on-line as proposed in [28]. All of these quantities can be updated dynamically as the data is processed and passed to the display for visualization. Two thresholds for alarms are set at $\Delta V_5/\Delta P_{53} = 0.08$, for an early warning signal (yellow dash–dot line), and $\Delta V_5/\Delta P_{53} = 0.24$, for a final alarm (red dash–dot line). A similar screenshot of $\Delta V_5/\Delta Q_{53}$ can be done in the similar way.

To explain how this wide-area early warning monitoring tool works, two screenshots of $\Delta V_5/\Delta Q_{53}$ (Case **1.1** in Section 5.3) at two different times (**I** at $t = 240$ s and **II** at $t = 360$ s) are captured and combined as shown in Figure 17. The voltage instability scenario is implemented by increasing load at Bus 5 as explained earlier. The load increase raises the value of the sensitivities. This in turn changes the colors of the contour map. This color corresponds to the sensitivity values. The selected QV-curve (of Bus 5, in this case) changes its value decreasingly when the load increases. Before the system collapses, an early warning signal can be generated by setting different threshold values. In the illustration in Figure 17, an early warning signal (yellow) can be generated when $\Delta V_5/\Delta Q_{53} = 0.2$ (at $t = 240$ s) and a final alarm signal (red) in case $\Delta V_5/\Delta Q_{53} = 0.6$ (at $t = 360$ s), respectively. The traffic light in the monitor will change colors accordingly. Thus, the proposed approach is capable of providing an early warning even earlier, e.g. at $t = 160$ s since the value of $\Delta V_5/\Delta Q_{53}$ changes from positive to negative at $t = 400$ s (while the system collapses at $t = 440$ s); however, we have set a conservative threshold for our illustration.

7. CONCLUSIONS AND FUTURE WORK

This article has described an approach for using voltage sensitivities computed from synchrophasor data, and a visualization approach that can be implemented for wide-area VS monitoring to be used in wide-area early warning systems. If implemented for control room use, this monitoring tool can be used by system operators in order to track the states of power system during normal and severe operating conditions.

The idea behind this approach is to ease system operators' tasks by automatically generating early warning signals before a collapse occurs. To achieve this, sensitivities calculated from voltage phasors are utilized as stability indicators. Different system conditions are determined by the sensitivities which need to be computed from filtered synchrophasor measurement data. The filtering approach is effective in sorting out unwanted electromechanical oscillations, noise and outliers before computing the sensitivities. Both visualization and filtering approaches are validated by using positive-sequence simulations, PMU-data from an RT-HIL and PMU-data from a real transmission system.

The most important lesson to share from this experience is that any PMU-data application for WAMS, and especially early warning systems, must be thoroughly tested with *actual* PMU measurements to

DOI: 10.1002/etep

guarantee its robustness. The effects of inherent data characteristics will require algorithms to cater for relevant features which are simply not present from traditional positive-sequence simulations. To this end, the use of an RT-HIL laboratory has been shown to be very advantageous in case a real data is not available.

There are several issues that must be further addressed, including but not limited to: optimal filter design for sensitivity computations, base-lining for determining thresholds for different voltage instability indicators, etc. The ultimate goal is not only to have real-time visualization of power systems and early warnings, but also to use these sensitivities to automate certain actions of existing controllers in the power system before the PMU-data is centralized in the control room.

8. LIST OF SYMBOLS AND ABBREVIATIONS

8.1. Symbols

V_i voltage magnitude at Bus i
I_{ik} current magnitude from from Bus i to Bus k.
δ_i voltage angle at Bus i.
δ_{ik} voltage angle difference between Bus i and Bus k.
$\overline{S}_{ik}$ complex power transmitted from Bus i to Bus k.
P_{ik} transmitted real power from Bus i to Bus k.
Q_{ik} transmitted reactive power from Bus i to Bus k.
$\delta_{P_{ik}}$ partial derivatives of voltage angle at Bus i with respect to active power flow from Bus i to Bus k.
$\delta_{Q_{ik}}$ partial derivatives of voltage angle at Bus i with respect to reactive power flow from Bus i to Bus k.
$V_{P_{ik}}$ partial derivatives of voltage magnitude at Bus i with respect to active power flow from Bus i to Bus k.
$V_{Q_{ik}}$ partial derivatives of voltage magnitude at Bus i with respect to reactive power flow from Bus i to Bus k.
$\Delta\delta_i$ voltage angle difference between present time step compares to previous time step at Bus i.
ΔV_i voltage magnitude difference between present time step compares to previous time step at Bus i.
ΔP_{ik} active power flow (from Bus i to Bus k) difference between present time step compares to previous time step.
ΔQ_{ik} reactive power flow (from Bus i to Bus k) difference between present time step compares to previous time step.
$\delta_{Q_{ik}}$ partial derivatives of voltage angle with respect to reactive power.
P_{L0} initial base active power.
Q_{L0} initial base reactive power.
λ active loading factor.
β reactive loading factor.

8.2. Abbreviations

RT	real-time
HIL	hardware-in-the-loop
PMU	phasor measurement unit
WAMPAC	wide-area monitoring, protection and control
WAMS	wide-area monitoring systems
VS	voltage stability
PSB	positive-sequence-based
MA	moving average
OLTC	on-load tap changer
OEL	over excitation limiter
PTs	potential transformers
CTs	Current transformers

DOI: 10.1002/etep

ACKNOWLEDGEMENTS

This work was supported in part by the EU funded FP7 iTesla project; the STandUP for Energy collaboration initiative; by Statnett SF, the Norwegian Transmission System Operator; and Nordic Energy Research through the STRONgrid project.

REFERENCES

1. Terzija V, Valverde G, *et al*. Wide-Area Monitoring, Protection, and Control of Future Electric Power Networks. *Proceedings of the IEEE* 2011; **99**:80–93.
2. Phadke A, Moraes R. The Wide World of Wide-area Measurement. *IEEE Power and Energy Magazine* 2008; **6**:52–65.
3. Bose A. Smart Transmission Grid Applications and Their Supporting Infrastructure. *IEEE Transactions on Smart Grid* 2010; **1**:11–19.
4. Zhang Y, Markham P, *et al*. Wide-Area Frequency Monitoring Network (FNET) Architecture and Applications. *IEEE Transactions on Smart Grid* 2010; **1**:159–167.
5. Zuo J, Carroll R, *et al*. Development of TVA SuperPDC: Phasor applications, tools, and event replay. *IEEE Power and Energy Society General Meeting* 2008.
6. Hauer A, Trudnowski D, *et al*. A Perspective on WAMS Analysis Tools for Tracking of Oscillatory Dynamics. *IEEE Power Engineering Society General Meeting* 2007.
7. Trudnowski D, Pierre J, *et al*. Performance of Three Mode-Meter Block-Processing Algorithms for Automated Dynamic Stability Assessment. *IEEE Transactions on Power Systems* 2008; **23**:680–690.
8. Parashar M, Mo J. Real Time Dynamics Monitoring System (RTDMS): Phasor Applications for the Control Room. in *42nd Hawaii International Conference on System Sciences (HICSS '09)*, 2009.
9. Hauer J, DeSteese J. Descriptive Model of Generic WAMS. Pacific Northwest National Laboratory,Richland, WA., Tech. Rep., 2007.
10. Venkatasubramanian V, Xing L, *et al*. Overview of wide-area stability monitoring algorithms in power systems using synchrophasors. in *American Control Conference (ACC)*, 2011.
11. Glavic M, Van Cutsem T. Wide-Area Detection of Voltage Instability From Synchronized Phasor Measurements. Part I: Principle. *IEEE Transactions on Power Systems* 2009; **24**:1408–1416.
12. Glavic M, Van Cutsem T. Wide-Area Detection of Voltage Instability From Synchronized Phasor Measurements. Part II: Simulation Results. *IEEE Transactions on Power Systems* 2009; **24**:1417–1425.
13. Taylor C. *Power System Voltage Stability*. McGraw-Hill, 1994.
14. Vu K, Begovic M, *et al*. Use of local measurements to estimate voltage-stability margin. *IEEE Transactions on Power Systems* 1999; **14**:1029–1035.
15. Smon I, Verbic G, Gubina F. Local Voltage-Stability Index Using Tellegen's Theorem. *IEEE Transactions on Power Systems* 2006; **21**:1267–1275.
16. Vournas C, Sakellaridis N. Tracking Maximum Loadability Conditions in Power Systems. in *iREP Symposium Bulk Power System Dynamics and Control - VII. Revitalizing Operational Reliability*, 2007.
17. Milosevic B, Begovic M. Voltage-stability protection and control using a wide-area network of phasor measurements. *IEEE Transactions on Power Systems* 2003; **18**:121–127.
18. Bao L, Huang Z, Xu W. Online Voltage Stability Monitoring Using Var Reserves. *IEEE Transactions on Power Systems* 2003; **18**:1461–1469.
19. Glavic M, Van Cutsem T. Investigating state reconstruction from scarce synchronized phasor measurements. In 2011 *IEEE Trondheim PowerTech*, 2011.
20. Van Cutsem T. An approach to corrective control of voltage instability using simulation and sensitivity. *IEEE Transactions on Power Systems*1995; **2**: 616–622.
21. Begovic M, Phadke AG. Control of voltage stability using sensitivity analysis. *IEEE Transactions on Power Systems* 1992; **7**:114–123.
22. Higgins W. A Comparison of Complementary and Kalman Filtering. *IEEE Transactions on Aeospace and Electronic Systems* 1975; **AES-11**:321–325.
23. Smith SW. *The Scientist and Engineer's Guide to Digital Signal Processing*. California Technical Pub, 1997.
24. Leelaruji R, Vanfretti L. Detailed Modelling, Implementation and Simulation of an 'All-in-one' Stability Test System including Power System Protective Devices. *Simulation Modelling Practice and Theory, Elsevier* 2012; **23**:36–59.
25. Vanfretti L, *et al*. SmarTS Lab - A Laboratory for Developing Applications for WAMPAC Systems. in *IEEE PES General Meeting*, 2012.
26. Van Cutsem T, Vournas C. *Voltage Stability of Electric Power Systems*. Kluwer Academic Publishers, 1998.
27. Corsi S, Taranto G. Voltage instability - the different shapes of the "Nose"," in *iREP Symposium Bulk Power System Dynamics and Control - VII. Revitalizing Operational Reliability*, 2007.
28. Parniani M, Chow JH, *et al*. Voltage Stability Analysis of a Multiple-Infeed Load Center Using Phasor Measurement Data," in *IEEE PES Power Systems Conference and Exposition (PSCE '06)*, 2006.

DOI: 10.1002/etep